Biophysical Characterization of the DNA Binding and Condensing Properties of Adenoviral Core Peptide μ (mu)†

Michael Keller,* Toshiaki Tagawa, Monika Preuss, and Andrew D. Miller*

Department of Chemistry, Imperial College Genetic Therapies Centre, Flowers Building, Armstrong Road, South Kensington, London SW7 2AZ, U.K.

Received August 1, 2001

ABSTRACT: Cationic peptides containing Lys and Arg residues interact with DNA via charge−charge interactions and are known to play an important role in DNA charge neutralization and condensation processes. In this paper, we describe investigations of the interaction of the cationic adenovirus core complex peptide μ (mu) with a dodecameric ODN (12 bp) and pDNA (7528 bp) using a combination of fluorescence spectroscopy, circular dichroism spectroscopy, isothermal titration calorimetry, and photon correlation spectroscopy. Comparisons are made with protamine, a cationic peptide well-known for DNA charge neutralization and condensation. Equilibrium dissociation constants are derived independently by both CD and ITC methods for the interaction between protamine or mu with pDNA ($K_d = 0.6-1$ μM). Thermodynamic data are also obtained by ITC, indicating strong charge−charge interactions. The interaction of protamine with pDNA takes place with decreasing entropy (−28.7 cal mol^{-1} K^{-1}); unusually, the interaction of mu with pDNA takes place with increasing entropy ($\Delta S°_{bind} = 11.3$ cal mol^{-1} K^{-1}). Although protamine and mu appear to destabilize pDNA double helix character to similar extents, according to CD thermal titration analyses, PCS studies show that interactions between mu and pDNA result in the formation of significantly more size-stable condensed particles than protamine. The enhanced flexibility and size stability of mu−DNA (MD) particles (80−110 nm) compared to protamine counterparts suggest that MD particles are ideal for use as a part of new nonviral gene delivery vectors.

The process of selective molecular recognition and binding of DNA by proteins and/or peptides is governed by a hierarchy of interactions involving amino acid side chains (*1*). Three types of interaction account for selective molecular recognition and binding. These are (i) stacking interactions between aromatic side chains, such as the indole moiety of Trp (*2*) or the aromatic side chains of Phe and Tyr, and DNA bases (*3*, *4*); (ii) hydrogen bonding interactions between hydrophilic side chains (Tyr, Asn, Ser, Thr, and His) and nucleotides; and (iii) ionic interactions involving positively charged side chains (Arg, Lys, and His) and the phosphodiester backbone of DNA. All three types of interactions are sequence-dependent with respect to both DNA and peptide and/or protein sequences. Cationic peptides usually make use of ionic interactions for molecular recognition and binding of DNA.

Cationic peptides are frequently used to charge-neutralize and condense DNA to form compact toroids (*5*) or rod structures (*6*, *7*). Toroid formation can apparently be achieved with trivalent cations (*8*), spermidine (*9*) protamine (*10*), poly(L-lysine) (*11*), polyethyleneimine (*12*), and even positively charged surfaces (*13*). Efficient DNA condensation and neutralization is a necessary prerequisite for cationic liposome-mediated gene delivery (lipofection) (*14*). Therefore, several different cationic peptides have been used to try to enhance cationic liposome-mediated gene delivery. For instance, oligo- and poly(L-lysine) (*15*, *16*), or more importantly protamine (*10*, *17*, *18*), have frequently been found to enhance lipofection severalfold (*19*). More recently, switch peptides have been reported which undergo conformational changes when exposed to pH changes of ∼2 pH units, which is useful for enhancing nucleic acid trafficking in cells and hence promoting lipofection efficiency (*20*). Because of the potential importance of cationic peptides in gene delivery, we have become interested in the biophysical characterization of interactions between cationic peptides and nucleic acids for two reasons. By performing studies of this type, we have been aiming at first understanding more about the biological function of these cationic peptides per se and second identifying physical characteristics that may be beneficial for nonviral gene therapy applications.

In this work, we describe the results of a direct comparison between protamine and the μ[1] (mu) peptide (Figure 1). Protamine is a naturally occurring peptide found in the head of spermatozoa. The role of protamine is to condense DNA

† M.K. thanks the Swiss National Science Foundation (SNF) for supporting this work (Grants 83EU-056143 and SNF1070). We thank Mitsubishi Chemical Corp./Mitsubishi-Tokyo Pharmaceuticals for supporting the Imperial College Genetic Therapies Centre.

* To whom correspondence should be addressed: Department of Chemistry, Imperial College Genetic Therapies Centre, Flowers Building, Armstrong Road, Imperial College of Science, Technology and Medicine, South Kensington, London SW7 2AZ, U.K. E-mail: mike.keller@ic.ac.uk or a.miller@ic.ac.uk. Telephone: ++44 (0)20 7594 3156. Fax: ++44 (0)20 7594 5803.

[1] Abbreviations: CD, circular dichroism; ds, dansyl; HEPES, *N*-(2-hydroxyethyl)piperazine-*N*′-2-ethanesulfonic acid; ITC, isothermal titration calorimetry; μ, mu peptide; ODN, oligonucleotide; pDNA, plasmid DNA; PA, protamine; PCS, photon correlation spectroscopy.

10.1021/bi0156299 CCC: $22.00
Published on Web 12/18/2001

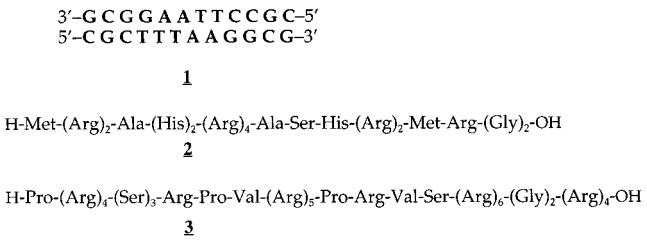

FIGURE 1: Molecular structures investigated in this study: oligo-DNA (ODN) **1**, adenoviral core peptide mu **2**, and protamine (PA) **3**.

in sperm and aid in DNA transfer to the egg nucleus (*10*). The mu peptide derives from the adenovirus core complex (*21*), where there may be up to 125 copies per virion (*22*). Mature adenovirus consists of an icosahedral, nonenveloped capsid particle (approximately 90 nm) enclosing a core complex. The latter consists of a linear dsDNA viral genome (~36 kbp) noncovalently associated with two cationic proteins [proteins V (pV) and VII (pVII)] and the 19-amino acid mu peptide. There is as yet no clear, detailed picture concerning the core structure, and little understanding of the relative contributions of pV, pVII, and mu peptide to the process by which viral DNA is delivered into the host cell nucleus. However, evidence begins to suggest that pVII and mu peptide are most tightly associated with viral DNA, while pV may play a role in assisting the delivery of the adenovirus core complex into the host cell nucleus (*23*, *24*).

Mu and protamine are found to have different levels of interaction with a palindromic ODN model system (Figure 1), but very similar types of interaction with plasmid DNA. Nevertheless, subtle differences are identified between mu and protamine interactions with pDNA that may suggest a role for mu peptide in the development of new nonviral vectors for gene therapy.

EXPERIMENTAL PROCEDURES

Peptides. Mu peptide was synthesized by standard Fmoc-based Merrifield solid phase peptide chemistry on Wang resin (*25*). The synthesis proved to be difficult and required double couplings and deprotection steps. The pseudo-proline method was applied to prevent potential aggregation of the highly hydrophobic protected peptides during solid phase assembly, thereby improving the yield of the pure peptide. In this, the Ala-Ser dipeptide sequence was coupled as a temporary oxazolidine dipeptide building block (*26*, *27*). The pseudo-proline unit has been demonstrated to afford peptide with high purity and yield especially for difficult sequences (*28*). Dansyl chloride (Sigma-Aldrich, Steinheim, Germany) was coupled on resin using standard peptide protocols. Peptide purification was carried out on a Hitachi semipreparative HPLC system at a flow rate of 30 mL/min, using a LiChrospher C_{18} (300 Å, 5 μm) column. Analytical HPLC was carried out on a Hitachi system using a Purospher RP-18 end-capped column (5 μm) at a flow rate of 1 mL/min, with a gradient from 0 to 100% acetonitrile (20 min). All peptides were analyzed by mass spectrometry (MALDI) and analytical HPLC before use. Salmon protamine (free base) was purchased from Sigma-Aldrich and used without further purification after its purity had been verified by analytical HPLC. All peptides described herein were analytically pure (>95%, analytical HPLC), and mu peptide was desalted on Sephadex G-25 M (PD 10) columns (Amersham Pharmacia Biotech, Uppsala, Sweden) after purification by semipreparative HPLC.

DNA. Single-stranded oligonucleotide was purchased from Oswell Research Products Ltd. (Southampton, U.K.) and annealed to double-stranded ODN as indicated by the manufacturer. Plasmid DNA pNGVL1 was obtained from the University of Michigan Vector Core and amplified and purified by Bayou Biolabs. The concentration of pDNA was determined spectrophotometrically ($A_{260} = 1 \cong 50$ μg/mL), and pDNA or ODN molar concentrations were determined using the average nucleotide base pair molecular mass of 660 Da (*29*).

Fluorescence Binding Studies. Experiments were performed on a Shimadzu RF-5301 spectrofluorimeter, at 20 °C by means of a cryostated water bath (Grant LTD 6). *N*-Dansyl peptides (3 or 1.5 μM) in 4 mM HEPES buffer (pH 7.8) were titrated with ODN from 10 to 3000 nM. After each addition, the dansyl fluorescence emission spectrum was recorded between 400 and 460 nm, using an excitation wavelength of 323 nm and excitation and emission bandwidths of 3 nm. Fluorescence emission intensities at 540 nm were corrected for any residual ODN background, and the emission intensity of free peptide (i.e., in the absence of ODN) was subtracted to give the fluorescence intensity enhancement, ΔI_{540}, due to the interaction of the peptide with ODN at each individual ODN concentration. All measurements were carried out in triplicate. ΔI_{540} values were fitted where appropriate by means of the McGhee−von Hippel isotherm (*30*) (eq 1):

$$K_d = \frac{1}{[L_F]} \frac{\nu}{1 - n\nu} \left[\frac{1 - (n-1)\nu}{1 - n\nu}\right]^{n-1} \quad (1)$$

where ν equals [PL]/[P_o], the molar ratio of the receptor-bound ligand L concentration ([PL]) to the total receptor concentration ([P_o]), and n is an overlap-site parameter which describes the coverage of lattice phosphate units per molecule ligand (*30*−*33*). The free ligand concentration was determined as described by Gatto et al. (*33*).

Circular Dichroism Binding Experiments. Circular dichroism (CD) experiments were performed using a JASCO J-715 spectropolarimeter (Beckmann-Coulter) at 20 °C. ODN (14.6 μM) or pDNA (phosphate concentration of 166 μM) in 4 mM HEPES buffer (pH 7.8) was titrated with peptide from 0.40 to 2.8 μM. CD spectra were recorded between 220 and 350 nm using a step resolution of 0.2 nm, a scan speed of 10 nm/min, a bandwidth of 1 nm, and a sensitivity of 10 mdeg. All measurements were carried out in duplicate and averaged to one single curve. In the case of pDNA, CD signal intensities at 273 nm, ΔOD_{273}, were corrected by subtraction of the signal intensity of free pDNA (i.e., in the absence of peptide) to give the CD intensity change, $\Delta\Delta OD_{273}$, due to the interaction of the peptide with pDNA at each individual peptide concentration. The mu peptide showed no significant CD signal at 273 nm; therefore, no peptide background correction was needed. $\Delta\Delta OD_{273}$ values were then fitted where appropriate by means of the McGhee−von Hippel isotherm (eq 1), as described above. The free ligand concentration was determined from ellipticity isotherms obtained from a series of different [PL]:[P_o] ratios as described in detail by Durand and Hélène (*32*). The associa-

tion constant K_a was extracted from the intercept with the *y*-axis of a linear graph obtained by the combination of four independent data sets. The overlap-site parameter *n* was obtained from the intercept of the same linear curve from the *x*-axis. Standard deviations were calculated from the deviation coefficient of the fitted linear graphs (*30*). Raw ellipticity data were converted into optical density (OD) units by using the relation $\Theta = \Delta A \times 33000$.

Isothermal Titration Calorimetry Experiments. Binding studies were performed by isothermal titration calorimetry (ITC) using a VP-ITC microcalorimeter from MicroCal (Northampton, MA). Titration data were processed by means of the Origin software provided by the manufacturer. Baseline corrections were used for the endothermic aggregation phases to permit the fitting of data points to a single-affinity binding site model (*34*). In the case of ITC experiments with the ODN, peptide (10 or 20 μM) was maintained in the thermostated cell (2 mL) at 20 °C in 4 mM HEPES (pH 7.8), and the whole was stirred at 350 rpm. ODN was introduced into the stirred cell by means of a syringe via 25 individual injections [each injection was 10 μL containing ODN (10 or 20 μM) in 4 mM HEPES (pH 7.8)]. Injections were 12 s in duration, and individual injections were programmed at intervals of 240 s. Samples were degassed at 10 °C in a ThermoVac system (MicroCal) prior to use. All experiments were carried out in triplicate using different concentrations for both DNA and peptide. Data were processed as described above and fit where appropriate using a single-affinity binding site model by nonlinear least-squares analysis. ITC experiments with pDNA were performed in reverse. pDNA (17.5 or 22 nM) was maintained in the thermostated cell (2 mL) at 20 °C in 4 mM HEPES (pH 7.8), and the whole was stirred at 350 rpm. Peptide was introduced into the stirred cell by means of a syringe in 25 ($\times$10 μL) or 45 ($\times$5.5 μL) individual injections [each injection containing peptide (410 μM) in 4 mM HEPES (pH 7.8)].

CD Temperature Titration Experiments. pDNA melting profiles were analyzed by CD spectroscopy. pDNA (6 nM) in 4 mM HEPES (pH 7.8) was heated in a thermostated CD cell at a rate of 1 °C/min from 20 to 95 °C. The CD signal at 273 nm, ΔOD_{273}, was observed as a function of temperature in the presence (0.001 equiv) and absence of peptides. Melting temperatures, T_m, were determined using the graphical analysis program Origin version 5.

Photon Correlation Spectroscopy. pDNA (approximately 1 mg/mL) was added to vortex-mixed, dilute solutions of peptide (0.1 mg/mL) in 4 mM HEPES (pH 7.8) to give a final pDNA concentration of 24 μg/mL. Particle sizes were measured by photon correlation spectroscopy using an N4 plus MD submicron particle analyzer (Beckman Coulter, High Wycombe, Buckinghamshire, U.K.). All measurements were performed at 20 °C, and all data were recorded at 90°, with an equilibration time of 1 min and individual run times of 300 s. The refractive index of the buffer was set to 1.333. Unimodal analysis was used throughout to calculate the mean particle size and standard distribution in four separate experiments.

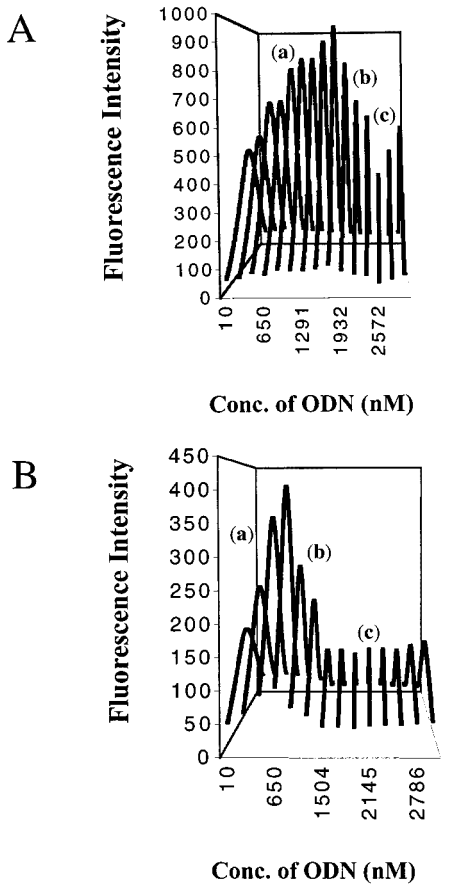

FIGURE 2: Reverse titrations of *N*-dansyl-labeled mu (ds-mu) with ODN. The fluorescence intensity graphs at different peptide:pDNA ratios are pictured from the side in three dimensions for a better view of the relative intensity changes: (A) [ds-mu] = 3 μM and (B) [ds-mu] = 1.5 μM. The ODN concentration was augmented in 15 separate titrations each increasing the ODN concentration 214 nM until a stoichiometric ratio of 1:1 (mu:ODN) was reached at 1500−1600 nM (A) and 700−800 nM (B) (a). When continuing addition of ODN, the 2:1 complex (mu_2−ODN) dissociates into two 1:1 complexes (mu−ODN) (b) until saturation, i.e., until complete dissociation of all 2:1 complexes to 1:1 complexes is reached (c).

RESULTS

Interaction of Peptides with d(GCGGAATTCCGC)

Fluorescence Spectroscopy. Preliminary binding studies with μ (mu) peptide were carried out using the palindromic oligonucleotide (ODN) sequence d(GCGGAATTCCGC). For this purpose, a reverse titration method was employed in which a constant concentration of *N*-dansyl mu peptide (3 or 1.5 μM) was titrated with ODN (Figure 2). The binding of ODN to *N*-dansyl peptide was assessed by observing changes in the fluorescence emission intensity, ΔI_{540}, of the dansyl group as a function of ODN concentration. Binding isotherms could be divided into two phases. In the low ODN concentration range, emission intensities were seen to increase with ODN concentration and the fluorescence emission maximum was seen to undergo a blue shift (from 540 to 529 nm). This is consistent with a situation in which the dansyl group exhibits an increase in fluorescence quantum yield as a result of binding interactions that place the dansyl group in a more hydrophobic environment than before, protected from collisional solvent quenching of fluorescence emission intensity. The ODN consists of two

strands, each presenting 11 negative charges from phosphodiester links. At pH 7.8, mu peptide has nine positive charges from nine Arg residues; hence, each ODN should be able to bind one mu peptide per strand. Accordingly, in this low-concentration regime, we would suggest that equilibria were seen to be associated with the formation of 2:1 mu−ODN complexes. Furthermore, fluorescence emission intensity associated with the first phase of each binding isotherm was found to peak at an approximately 2:1 molar ratio, a result that is consistent with this argument.

During the second phase of each binding isotherm associated with the higher ODN concentration range, emission intensities were seen to decrease with ODN concentration but without a significant shift in the fluorescence emission maximum. This may be attributed to a decrease in the fluorescence quantum yield with binding because of a progressive equilibrium shift toward 1:1 mu−ODN complexes as the ODN concentration continues to increase. Consistent with this argument, no further changes in fluorescence intensity or emission maximum were observed above a 1:1 mu:ODN molar ratio (Figure 2). First-phase fluorescence binding data were fitted with the McGhee−von Hippel isotherm to estimate an observed equilibrium dissociation constant, K_d, for the interaction between the dansyl-labeled mu peptide and the ODN. A K_d value of 0.8 μM was determined together with an overlap-site parameter n of 8−9 (where n is the number of phosphates covered by the peptide). The value of n is in agreement with the fact that mu peptide exhibits nine positive charges from nine Arg residues at pH 7.8, each of which can complement a single phosphodiester link. Furthermore, the value of K_d is consistent with results obtained from other systems known to interact primarily by charge−charge interactions (*33*).

A titration of a fixed concentration of *N*-dansyl-labeled protamine with ODN gave results that were very different from the results of the titration with the *N*-dansyl-labeled mu peptide. Protamine appeared to induce aggregation of the ODN too readily so that we were forced to abandon the titration experiment.

Circular Dichroism. Circular dichroism of ODN gave a characteristic spectrum with a minimum at 220 nm and a maximum at 284 nm. We attempted the titration of a fixed concentration of ODN with mu peptide and observed a decrease in the amplitude of the CD signal at 284 nm in the low mu peptide concentration range (0−0.15 mu:ODN molar ratio) (Figure 3). However, aggregation and precipitation were observed as the mu peptide concentration was increased further. This is consistent with an initial phase of peptide binding by strong electrostatic interactions in which there is a progressive loss of ODN double-helical character, accompanied by partial solvent exposure of hydrophobic base pairs, followed by aggregation as charge neutrality is approached (*32*). A titration of a fixed concentration of ODN with protamine gave similar results. Unfortunately, in neither case were sufficient data points obtained prior to aggregation to plot a saturation binding isotherm using CD titration data to corroborate the value of the equilibrium dissociation constant obtained by fluorescence spectroscopy.

Isothermal Titration Calorimetry. The interaction between native (nondansylated) mu peptide and the ODN was also analyzed by ITC. A fixed concentration of mu peptide (10 or 20 μM) was titrated in 4 mM HEPES buffer (pH 7.8)

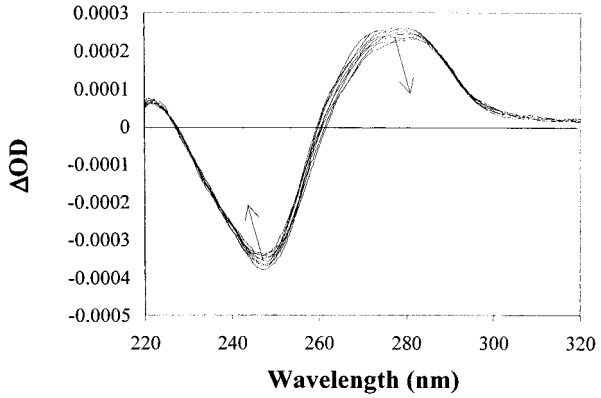

FIGURE 3: Circular dichroism spectrum of pDNA (11 nM) in complex with varying amounts of mu peptide (0−4.1 μM). A progressive increase in peptide concentration is accompanied by a linear decrease in the CD amplitude at 273 nm which can be used to derive an association constant for low peptide:pDNA ratios.

with ODN in 25 separate injection steps (data not shown). The output could be divided into two distinct phases. These were (i) a sigmoidal exothermic phase characteristic of a normal binding process and (ii) an endothermic phase that could be ascribed to aggregation processes. A single-affinity binding site model was used to fit the first sigmoidal phase, giving an equilibrium dissociation constant, K_d, of 0.013 ± 0.010 μM. The enthalpy of binding, ΔH°_{bind}, was found to be −55 ± 0.04 kcal/mol, the entropy, ΔS°_{bind}, −153 cal mol^{-1} K^{-1}, and the average number of ODNs per peptide, N, 0.35. The latter suggests that two to three mu peptides bound per ODN molecule, confirming results obtained from the fluorescence titration binding experiment (see above). There is a clear 1 order of magnitude discrepancy between equilibrium dissociation constants determined by ITC and those determined by fluorescence. This difference most likely reflects the difference in affinity between mu and *N*-dansyl-labeled mu peptides for the ODN, the dansyl group partially inhibiting or occluding the interaction of the mu peptide in some way, thereby reducing the affinity of peptide for ODN by at least 1 order of magnitude. As described previously, interactions between ODN and protamine proved to be difficult to study because of the ease of aggregation, so we were forced to abandon the titration experiment at concentrations of ODN that were too low to obtain a complete sigmoidal phase, thereby preventing adequate derivation of the binding constants.

Interaction of Peptides with pDNA

The strong affinity of both mu and protamine for ODN was established but difficult to quantify due to aggregation, and interactions between mu or protamine and pDNA harboring the β-galactosidase reporter gene were studied. This study was carried out in an effort to establish whether mu is a compound suitable for binding and condensing pDNA for use in nonviral gene delivery. Protamine has been used as a pDNA condensing agent in the development of lipid−peptide−pDNA ternary systems for use in gene delivery (*10*, *18*, *35*). Therefore, given this relevance to gene delivery, a comparison was made between mu and protamine interactions with pDNA.

Circular Dichroism. Using a fixed concentration of pDNA, the binding of either mu peptide or protamine to pDNA was

Table 1: Parameters of Peptide Binding to pDNA As Determined by Isothermal Titration Calorimetry and Circular Dichroism Spectroscopy at 293 K in 4 mM HEPES (pH 7.8)

peptide	$\Delta H°_{bind}$ (kcal/mol)[a]	$\Delta S°_{bind}$ (cal mol^{-1} K^{-1})[a]	K_d (μM)[a]	N (no. of ligands/ plasmid)[a]	K_d (μM)[b]	n[b,c]
mu	-5 ± 0.1	11.3	0.6 ± 0.1	1200−1400	0.8 ± 0.3	32 ± 4
protamine[a]	-16.5 ± 1.6	−28.7	1 ± 0.7	400−450	0.6 ± 0.02	85 ± 2

[a] Measured by ITC at 293 K. [b] Derived from data obtained by CD spectroscopy by fitting initial linear data at low peptide:pDNA ratios to the McGhee−von Hippel isotherm using linear regression. [c] Overlap-site parameter derived from the McGhee−von Hippel isotherm using linear regression.

monitored by observing changes in ΔOD_{273} as a function of peptide concentration (Figure 3). Added peptide made no spectral contribution at 273 nm; therefore, all changes in ΔOD_{273}, $\Delta\Delta OD_{273}$, relative to the initial pDNA signal could be confidently assigned to changes in pDNA structure as a result of peptide binding as described for similar systems (*32*, *36*). $\Delta\Delta OD_{273}$ values were plotted as a function of the peptide concentration and the data fitted with the McGhee−von Hippel isotherm assuming single affinity binding sites (see above). Initial binding events for low peptide:pDNA ratios are linear when represented in a Scatchard plot but exhibit typical curvatures for higher ratios (*30*). Therefore, for the calculation of binding parameters, only initial values must be used. This analysis afforded an overall observed K_d of 0.8 ± 0.3 μM for the interaction of mu peptide and pDNA with an overlap-site parameter n of 32 ± 4 (Table 1). Protamine exhibited a very similar macroscopic affinity, although with a much bigger overlap-site parameter n of 85 ± 2.

Isothermal Titration Calorimetry. A fixed concentration of pDNA (17.5 or 22 nM) was titrated with mu peptide [26 injections (10 μL) of a 410 μM peptide solution], giving a mainly biphasic output similar to that obtained with mu peptide (Figure 4A) and the ODN. The first phase was a characteristic exothermic binding phase exhibiting a sigmoidal shape followed by an endothermic second phase suggestive of pDNA condensation and subsequent aggregation, which is known to be triggered usually when a 90% charge equivalent of a cationic species is combined with pDNA (*6*). As described previously, a single-affinity binding site model was used to fit the first sigmoidal phase (*34*), giving an overall K_d value of 0.6 ± 0.1 μM. Other thermodynamic data are given (Table 1). Most notably, $\Delta S°_{bind}$ was 11.3 cal mol^{-1} K^{-1} and the average number of mu peptides bound per plasmid, N, was estimated to be 1200−1400 (Table 1). This overall value of K_d is in excellent agreement with that value obtained for the interaction between mu peptide and pDNA via the CD binding titration experiment (see above). When the same experiments were performed with protamine, a similar overall K_d value was deduced but $\Delta S°_{bind}$ was found to be −28.7 cal mol^{-1} K^{-1} and the value of N was estimated to be $^1/_3$ of the number found with mu peptide (Table 1 and Figure 4B). In other words, while the interaction of mu peptide with pDNA was substantially driven by enthalpy and increase in system entropy as a result of binding, the interaction of protamine peptide with pDNA was exclusively driven by enthalpy.

CD Temperature Titrations. CD temperature titration experiments were performed to determine the impact of both mu and protamine on the pDNA melting temperature, T_m. The change in intensity of the pDNA ΔOD_{273} maximum was followed as a function of temperature in the presence and

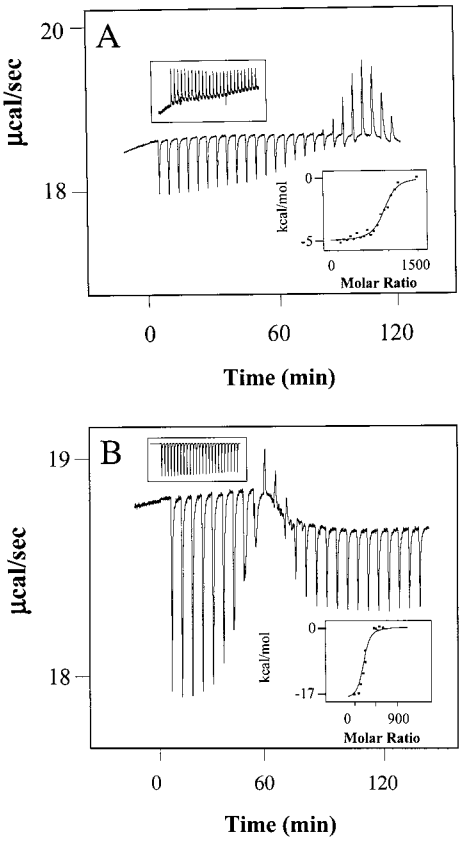

FIGURE 4: Thermodynamic profile obtained from isothermal titration calorimetry studies of the binding event between (A) mu and protamine (B) with pDNA. The insets at the top left are the energy of dilution of the peptides when injected into HEPES (pH 7.8, 4 mM). The insets at the bottom right are the curve fittings of the experimental data to a single-affinity binding site model using the least-squares method.

absence of peptides. Experiments were performed with peptide/pDNA mixtures comprising only low peptide:pDNA molar ratios to avoid interference and complications from peptide-induced pDNA condensation processes. In the absence of peptide, a sharp transition was observed with a midpoint inflection temperature, T_m, at 62 °C, characteristic of pDNA melting (base unstacking and loss of Watson−Crick hydrogen bond integrity). However, even in the presence of very small amounts of mu peptide (mu:pDNA, 0.001 equiv, w/w), the T_m was still shifted to a lower temperature of 59 ± 0.5 °C (hypochromic shift), consistent with peptide-induced destabilization of the DNA double helix (Figure 5). The same experiment conducted with protamine gave very similar results with a slightly lowered T_m of 59 ± 1 °C.

DNA Condensation. Continuous addition of a cationic peptide to pDNA is well-known to trigger a volumetric collapse of the DNA structure resulting in compact, con-

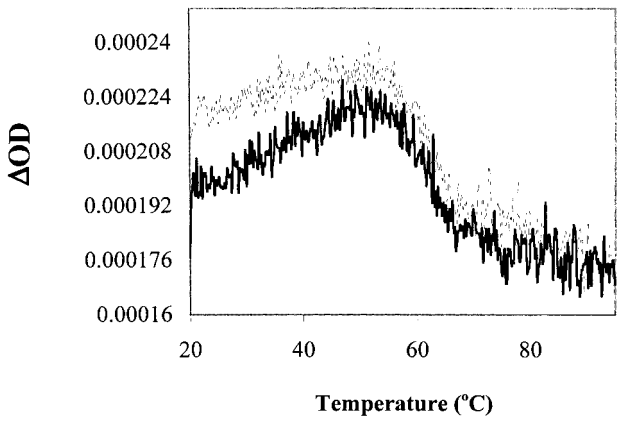

FIGURE 5: Representative example of pDNA melting experiments. The maximum CD absorbance at 273 nm for increasing temperatures (from 20 to 100 °C, at 1 °C/min) is shown. The dashed line (background) represents the absorbance profile of peptide-free pDNA over the indicated temperature range. The solid line is pDNA in complex with 0.001 equiv of mu peptide.

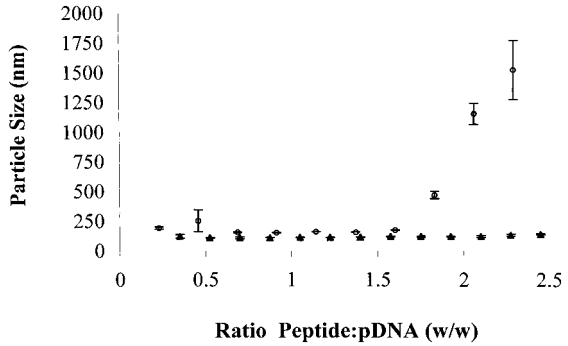

FIGURE 6: Results of photon correlation spectroscopy experiments. The particle sizes of peptide−pDNA complexes at different ratios with mu (▲) and protamine (○) were measured using the unimodal mode. Note that for peptide:DNA ratios exceeding 1.7, particles consisting of pDNA and protamine dramatically increase in size.

densed structures with defined structures (*6*, *7*). This process can be observed by photon correlation spectroscopy (PCS). PCS analyses were performed of a series of mixtures containing a fixed amount of pDNA and a variable amount of mu peptide (Figure 6).

Over a broad range of mu:DNA ratios (0.4−2.5, w/w), mu peptide was found to condense pDNA to form small, size-stable particles 80−110 nm in diameter. By contrast, protamine was found to condense pDNA to form small, size-stable particles over a narrower range of protamine:DNA (w/w) ratios (0.4−2.5). Protamine has approximately double the molecular weight and double the number of cationic amino acid residues (Arg and Lys) compared to mu peptide (Figure 1). For a given weight, both mu and protamine offer equivalent numbers of cationic charges. Therefore, mu peptide appears to be more versatile at pDNA condensation than protamine by virtue of forming stable complexes over a broad range of peptide:pDNA ratios. Charge neutralization was also demonstrated by electrophoretic mobility shift assays. For mu:pDNA ratios exceeding 0.7, complete retardation of pDNA in the well was observed (cf. Figure 7). The same was true for protamine. Above protamine:pDNA ratios of 0.7−0.8, the complex was completely retarded in the well.

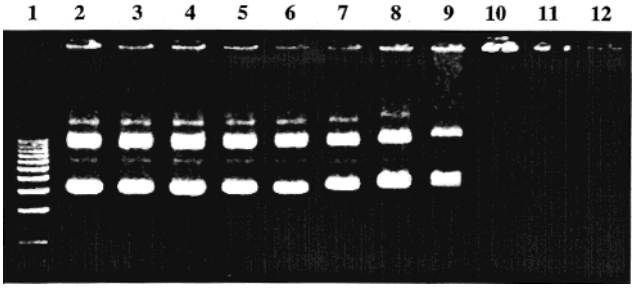

FIGURE 7: Electrophoretic mobility shift assay on agarose (1%) for varying mu:pDNA ratios: lane 1, 1 kb DNA ladder; lane 2, uncomplexed pDNA; and lanes 3−12, 0.1−1.0 peptide:pDNA ratios. Each lane represents a stepwise increase in the peptide:pDNA ratio of 0.1. It must be noted that for peptide:pDNA ratios exceeding 0.7 (lane 9), the peptide−pDNA complex is fully retained in the well.

DISCUSSION

The research described here represents a complete biophysical characterization of the interactions between mu peptide and nucleic acids, and a direct comparison between mu and another peptide well-known to interact with and condense DNA into small particles. Both peptides were extensively desalted before use to minimize any potential effects of salt on charge−charge interactions (*32*, *36*, *37*). There are some interesting differences in the abilities of the peptides to interact with DNA. Interactions between mu and the palindromic ODN were amenable to characterization, while those between protamine and the same ODN were not, because of aggregation problems. This may be the case because the ODN molecule was too short to allow adequate interaction with all the available protamine cationic charges. Protamine was observed to promote pDNA aggregation much more readily than mu peptide, perhaps by cross-linking (Figure 6) (*38*). The most effective comparison is between the relative affinities of mu and protamine for pDNA. Differences are subtle but nonetheless significant. Although overall K_d values were similar (0.6−1 μM) whether determined by ITC or CD titration binding experiments (Figures 3 and 4 and Table 1), approximately 3 times more mu than protamine bound with each pDNA as judged by ITC analysis. Therefore, if it is assumed that each peptide binding event is independent, individual site dissociation constants (*39*), κ_d, may be assessed using eq 2

$$\kappa_d = NK_d \quad (2)$$

Hence, values of κ_d for mu and protamine interactions with pDNA can be deduced as 780 and 430 μM, respectively, given respective peptide:pDNA molar ratios of 1300:1 and 430:1, and assuming ITC-derived K_d values for both. That site constants show protamine to bind with an affinity twice that of mu can be expected given the fact that protamine has approximately twice the number of cationic charges per mole as mu. Each pDNA molecule is comprised of 7528 bp and yields a total of 15 056 negative charges per plasmid. Hence, if we assume the peptide:pDNA molar ratios given above, mu peptide (nine Arg residues) is apparently neutralizing 80% of pDNA charge when pDNA binding is at saturation and protamine 60%. The difference in the "coverage" effected by the two peptides supports the above finding and may be further explained by the thermodynamic properties of the respective interactions.

The interaction of mu and pDNA appears to take place with an increase in system entropy, while that between protamine and pDNA appears to occur with a decrease in system entropy (Table 1). Usually, the binding of polycations to pDNA is accompanied by an initial disruption of the structured water layer around the phosphodiester backbone of pDNA, contributing to an increase in system entropy, followed by the formation of an alternative solvent cage around the resulting peptide−pDNA complexes leading to a loss of system entropy (*41*). This alternative solvent cage is believed to lack the polarity of the hydration shell of naked pDNA, causing elements of double helix to attract each other until the whole structure collapses into condensed particles with an even greater loss of system entropy (*6*, *42*). Parsegian and co-workers have suggested that condensing polycations assist the attraction process by provoking the rearrangement of surface-bound water in forming regions of hydration attraction or water bridging between double-helix regions (*43*). Some cationic systems may even create cross-links between double-helix regions as well, as shown by X-ray crystallography (*44*). Furthermore, this process may well be assisted by peptide binding-induced destabilization of pDNA double-helix elements as indicated by our CD temperature titration data (Figure 5). In agreement with these data, studies of the interaction of cationic lipids and pDNA using FTIR demonstrated that upon interaction with lipid, the pDNA remains in the B-form but is accompanied by considerable perturbation of the hydration structure (*45*). Hence, interactions between cationic peptides and pDNA should normally be expected to be accompanied by a decrease in system entropy as was observed for protamine−DNA interactions (Table 1). That interactions between mu and pDNA should be accompanied by an increase in system entropy suggests that mu−pDNA (MD) particles may be more flexible and structurally accommodating than their protamine counterparts, perhaps in part because mu is less able to form cross-links between double-helix regions of pDNA than protamine, since mu is only half the length and molecular weight of protamine (*44*). Alternatively, the mu peptide backbone may possess greater flexibility than the protamine backbone which harbors three proline residues that can limit the degree of conformational freedom due to steric repulsion of the cyclic Pro side chains (*40*). Both may not only explain why mu peptide was able to effect more extensive coverage of pDNA at saturation binding but also suggest why MD particles were more size-stable over a wider ratio range than corresponding protamine counterparts (Figure 6) (*38*). Furthermore, these steric constraints would account for why protamine induced ODN aggregation much more readily than mu peptide. Saturation binding of pDNA by mu was not accompanied by complete charge neutralization, which means that MD complexes have an overall negative charge following saturation binding.

Furthermore, if we assume that saturation binding corresponds to a mu:pDNA molar ratio of approximately 1300:1 as measured by ITC, this is equivalent to a mu:pDNA (w/w) ratio of approximately 0.6:1. Such a ratio should therefore be optimal for size-stable MD particle formation. Results of gel retardation assays confirm incomplete charge neutralization at mu:pDNA ratios of 0.6 (Figure 7). Salmon protamine has been used extensively to condense pDNA as part of ternary complexes for gene delivery such as the successful lipid−protamine−pDNA (LPD) nonviral vector systems reported by Huang and co-workers, and others (*10*, *17*, *18*, *46*−*50*). Given the subtle though important differences between mu and protamine, particularly the flexibility and size stability of the MD particles, the possibility that more effective liposome−mu−DNA (LMD) nonviral vector systems could be devised seems probable. We have made some progress in this regard and have recently described lipopolyplex systems involving mu peptide that appear to be able to transfect even postmitotic neuronal cells (*51*). On the basis of this work, results of the biophysical analyses described above, and an analysis of LPD systems, the design of an LMD prototype based around the optimal 0.6:1 (w/w) mu:pDNA ratio appears to be eminently possible and could represent an important new class of nonviral vector system.

In summary, mu peptide from the adenovirus core complex has proven to have strong affinities for both oligomeric and polymeric DNA. There are broad similarities between mu peptide and protamine in terms of pDNA binding affinities, but subtle differences particularly in the thermodynamics of binding and the stability of peptide−pDNA particles suggest that mu peptide may play a role in viral DNA packaging. Furthermore, its ease of formulation with pDNA over broad peptide:pDNA ratios renders this highly cationic peptide an ideal candidate for use in nonviral gene vector systems.

ACKNOWLEDGMENT

We thank Eric Perouzel for assisting in the mathematical evaluation of binding constants from the McGhee−von Hippel isotherm and Dr. Julian Tanner for helping with the ITC experiments and subsequent data analyses.

REFERENCES

1. Hélène, C. (1998) *Nature 391*, 436−438.
2. Rajeswari, M. R., Montenaygarestier, T., and Hélène, C. (1987) *Biochemistry 26*, 6825−6831.
3. Behmoaras, T., Toulmé, J. J., and Hélène, C. (1981) *Nature 292*, 858−859.
4. Behmoaras, T., Toulmé, J. J., and Hélène, C. (1981) *Proc. Natl. Acad. Sci. U.S.A. 78*, 926−930.
5. Schellmann, J. A., and Gosule, L. C. (1976) *Nature 259*, 333−335.
6. Bloomfield, V. A. (1996) *Curr. Opin. Struct. Biol. 6*, 334−341.
7. Golan, R., Pietrasanta, L. I., Hsieh, W., and Hansma, H. G. (1999) *Biochemistry 38*, 14069−14076.
8. Arscott, P. G., Li, A. Z., and Bloomfield, V. A. (1990) *Biopolymers 30*, 619−630.
9. Lin, Z., Wang, C., Feng, X. Z., Liu, M. Z., Li, J. W., and Bai, C. L. (1998) *Nucleic Acids Res. 26*, 3228−3234.
10. Li, S., and Huang, L. (1997) *J. Liposome Res. 7*, 207−219.
11. Laemmli, U. K. (1975) *Proc. Natl. Acad. Sci. U.S.A. 72*, 4288−4292.
12. Remy, J. S., Abdallah, B., Zanta, M. A., Boussif, O., Behr, J. P., and Demeneix, B. (1998) *Adv. Drug Delivery Rev. 30*, 85−95.
13. Fang, Y., and Hoh, J. H. (1998) *J. Am. Chem. Soc. 120*, 8903−8909.
14. Logan, J. J., Bebok, Z., Walker, L. C., Peng, S. Y., Felgner, P. L., Siegal, G. P., Frizzell, R. A., Dong, J. Y., Howard, M., Matalon, S., Lindsey, J. R., Duvall, M., and Sorscher, E. J. (1995) *Gene Ther. 2*, 38−49.
15. Colin, M., Harbottle, R. P., Knight, A., Kornprobst, M., Cooper, R. G., Miller, A. D., Trugnan, G., Capeau, J., Coutelle, C., and Brahimi-Horn, M. C. (1998) *Gene Ther. 5*, 1488−1498.

16. Deshmukh, H. M., and Huang, L. (1997) *New J. Chem. 21*, 113−124.
17. Sorgi, F. L., Bhattacharya, S., and Huang, L. (1997) *Gene Ther. 4*, 961−968.
18. Li, S., and Huang, L. (1997) *Gene Ther. 4*, 891−900.
19. Boulikas, T., and Martin, F. (1997) *Int. J. Oncol. 10*, 317−322.
20. Wyman, T. B., Nicol, F., Zelphati, O., Scaria, P. V., Plank, C., and Szoka, F. C. (1997) *Biochemistry 36*, 3008−3017.
21. Anderson, C. W., Young, M. E., and Flint, S. J. (1989) *Virology 172*, 506−512.
22. Hosokawa, K., and Sung, M. T. (1976) *J. Virol. 17*, 924−934.
23. Matthews, D. A., and Russell, W. C. (1998) *J. Gen. Virol. 79*, 1671−1675.
24. Zhang, W., Bond, J. P., Anderson, C. F., Lohman, T. M., and Record, M. T. (1996) *Proc. Natl. Acad. Sci. U.S.A. 93*, 2511−2516.
25. Merrifield, R. B. (1986) *Science 232*, 341−347.
26. Wöhr, T., Wahl, F., Nefzi, A., Rohwedder, B., Sato, T., Sun, X. C., and Mutter, M. (1996) *J. Am. Chem. Soc. 118*, 9218−9227.
27. Keller, M., Sager, C., Dumy, P., Schutkowski, M., Fischer, G. S., and Mutter, M. (1998) *J. Am. Chem. Soc. 120*, 2714−2720.
28. Keller, M., and Miller, A. D. (2001) *Bioorg. Med. Chem. Lett. 11*, 857−859.
29. Sambrook, J., Fritsch, E. F., and Maniatis, T. (1989) *Molecular Cloning: A Laboratory Manual*, Cold Spring Harbor Laboratory Press, Plainview, NY.
30. McGhee, J. D., and von Hippel, P. H. (1974) *J. Mol. Biol. 86*, 469−489.
31. Scatchard, G. (1944) *Ann. N.Y. Acad. Sci. 51*, 660−672.
32. Durand, M., Maurizot, J.-C., Borazan, H. N., and Hélène, C. (1975) *Biochemistry 14*, 563−570.
33. Gatto, B., Zagotto, G., Sissi, C., and Palumbo, M. (1997) *Biol. Macromol. 21*, 319−326.
34. Sigurskjold, B. W. (2000) *Anal. Biochem. 277*, 260−266.
35. Li, S., Rizzo, M. A., Bhattacharya, S., and Huang, L. (1998) *Gene Ther. 5*, 930−937.
36. Brun, F., Toulmé, J.-J., and Hélène, C. (1975) *Biochemistry 14*, 558−563.
37. Braunlin, W. H., and Bloomfield, V. A. (1991) *Biochemistry 30*, 754−758.
38. Keller, M., Preuss, M., Tagawa, T., and Miller, A. D. (2000) in *Peptides 2000* (Martinez, J., and Fehrentz, J.-A., Eds.) pp 487−488, EDK, Paris.
39. Hutchinson, J. P., Oldham, T. C., ElThaher, T. S. H., and Miller, A. D. (1997) *J. Chem. Soc., Perkin Trans. 2*, 279−288.
40. Wüthrich, K., Billeter, M., and Braun, W. (1984) *J. Mol. Biol. 180*, 715−740.
41. Dunitz, J. D. (1994) *Science 264*, 670.
42. Bloomfield, V. A. (1991) *Biopolymers 31*, 1471−1481.
43. Parsegian, V. A., Rand, R. P., and Rau, D. C. (2000) *Proc. Natl. Acad. Sci. U.S.A. 97*, 3987−3992.
44. Schellman, J. A., and Parthasarathy, N. (1984) *J. Mol. Biol. 175*, 313−329.
45. Choosakoonkriang, S., Wiethoff, C. M., Anchordoquy, T. J., Koe, G. S., Smith, J. G., and Middaugh, C. R. (2001) *J. Biol. Chem. 276*, 8037−8043.
46. Li, B., and Feng, S. (1999) *Biophys. J. 76*, A62.
47. Li, S., Tseng, W. C., Stolz, D. B., Wu, S. P., Watkins, S. C., and Huang, L. (1999) *Gene Ther. 6*, 585−594.
48. Chesnoy, S., and Huang, L. (2000) *Annu. Rev. Biophys. Biomol. Struct. 29*, 27−47.
49. Dokka, S., Toledo, D., Shi, X. L., Ye, J. P., and Rojanasakul, Y. (2000) *Int. J. Pharm. 206*, 97−104.
50. Birchall, J. C., Kellaway, I. W., and Gumbleton, M. (2000) *Int. J. Pharm. 197*, 221−231.
51. Murray, K. D., Etheridge, C. J., Shah, S. I., Matthews, D. A., Russell, W., Gurling, H. M. D., and Miller, A. D. (2001) *Gene Ther. 8*, 453−460.

BI0156299